JOURNAL OF SPACECRAFT AND ROCKETS
Vol. 31, No. 6, November-December 1994

Formulas for the Phase Characteristics in the Problem of Low-Earth-Orbital Debris

Joshua Ashenberg*
Chelmsford, Massachusetts 01863

Some formulas and relations for estimating the characteristics of the different phases in the problem of debris propagation are suggested. The methods are based on the assumption of a weak isotropic explosion as the orbital breakup mechanism. This assumption leads to a simple formulation of the torus, the apsidal, and the nodal closure times. A criterion that guarantees the separation of the atmospheric dissipation phase from the nodal dispersion is suggested as well.

Nomenclature

a = semimajor axis
$\boldsymbol{a}$ = orbital elements vector
A = particle reference area
C_D = drag coefficient
e = eccentricity
H = altitude
i = inclination
J_2 = second zonal harmonic of the Earth
M = mean anomaly
m = particle mass
n = mean orbital rate
R_E = Earth's equatorial radius
r = radius vector
T = orbital period
t = time
u = argument of latitude
V = speed
V_r = radial impulse
V_w = orthogonal impulse
V_θ = transverse impulse
δ = variation operator
$\boldsymbol{\delta}$ = Dirac delta function
ϑ = true anomaly
μ = geocentric gravitational constant
ρ = atmospheric density
Ω = latitude of ascending node
ω = argument of perigee

I. Introduction

THIS work deals with the dispersion of low-Earth-orbital debris, under the perturbations of the Earth's oblateness and the atmospheric drag. The breakup event is modeled as an isotropic explosion. The objective is to find simple formulations for the typical characteristics and the time orders of the propagation phases. It is customary to distinguish between the following four phases.[1]

Phases I and II are dominated by the two-body dynamics, whereas phases III and IV are due to the Earth's oblateness and the atmospheric drag, respectively. During phase I, which lasts only a few orbital revolutions, the ensemble of fragments forms a pulsating ellipsoid.[2] During phase II, the debris cloud spreads out to form a toruslike shape along the parent orbit. Phase III is dominated by the Earth's oblateness perturbations. The different apsidal and nodal drift rates cause a zonal dispersion that leads to a debris band that covers a part of the Earth and is confined in latitude depending on the parent inclination. Phase IV starts (ideally) after the band closure has been completed. This last phase is dominated by the atmospheric dissipation and leads finally to the "cleaning" via the orbital decay of the particles.

The main assumption is the restriction of the breakup to a weak, isotropic explosion. Thus, the initial condition for the dispersion will be formulated as a variation

$$\delta V = \boldsymbol{\delta}(\boldsymbol{r} - \boldsymbol{r}_0)\, \hat{V} \cdot \delta \boldsymbol{V} \tag{1}$$

where $\hat{V}$ is the unit vector along the nominal orbit. In view of Eq. (1), the instantaneous changes in the orbital elements, due to the velocity impulse at breakup, are well formulated by Poisson's method[3,4]:

$$\boldsymbol{\delta a} = \frac{\partial \boldsymbol{a}}{\partial \dot{\boldsymbol{r}}}\, \boldsymbol{\delta \dot{r}} + \boldsymbol{O} \tag{2}$$

The variations, due to the impulse at breakup, that are needed for further application are[4]

$$\delta a_j = \frac{2}{n\sqrt{1-e^2}}\left[\delta V_{r_j}\, e \sin\vartheta + \delta\, V_{\theta_j}(1 + e\cos\vartheta)\right]$$

$$\delta e_j = \frac{\sqrt{1-e^2}}{na}\left[\delta V_{r_j}\sin\vartheta + \delta V_{\theta_j}\frac{2\cos\vartheta + (1+\cos^2\vartheta)\, e}{1 + e\cos\vartheta}\right]$$

$$\delta i_j = \delta V_{w_j}\frac{\sqrt{1-e^2}\cos(\omega+\vartheta)}{na(1+e\cos\vartheta)} \tag{3}$$

These variations are evaluated for each particle j. Proceeding with this approach, phase III consists of an ensemble of a secular precessing ellipse, defined by the well-known kinematical relations[5]

$$\begin{aligned}
\bar{a}_j &= a_{0_j} \\
\bar{e}_j &= e_{0_j} \\
\bar{i}_j &= i_{0_j} \\
\bar{M}_j &= M_{0_j} + \bar{n}_j(J_2, a_{0_j}, e_{0_j}, i_{0_j})\,\Delta t \\
\bar{\omega}_j &= \omega_{0_j} + \dot{\omega}_j(J_2, a_{0_j}, e_{0_j}, i_{0_j})\,\Delta t \\
\bar{\Omega}_j &= \Omega_{0_j} + \dot{\Omega}_j(J_2, a_{0_j}, e_{0_j}, i_{0_j})\,\Delta t
\end{aligned} \tag{4}$$

where $\Delta t = t - t_0$.

Now, it is rather impractical to regard each particle separately. As we will see later on, it is sufficient to consider only a couple

Received Jan. 23, 1993; revision received July 22, 1993; accepted for publication July 23, 1993.

*Aerospace Scientist, P.O. Box 606. Member AIAA.

of particles. These will give the necessary information about each phase. A trivial and popular choice is the particles along the direction of the extreme orbital energy.[6,7] However, we will find that this is not always the most accurate way.

The following sections present some tools for a preliminary estimation of the dispersion phases. Phase I is not considered, since it has been solved explicitly, for circular orbits[6] as well as for eccentric orbits.[2] The discussion on the other phases is based on the assumption of small variations. The approach to phase III is based on the differential changes of the orbital elements.[8,9] Finally, a condition for separating phases III and IV is presented.

II. Phase II: Orbital Torus Closure

The pulsating ellipsoid of debris stretches out along the parent orbit due to different orbital rates among the ensemble of fragments. The variation of the orbital period δT is a function of the variation of the semimajor axis, which depends on the breakup impulse δV, i.e., $\delta T = \delta T(\delta V)$. Expanding the period difference, $\Delta T = \delta T + \frac{1}{2}!\delta^2 T + \cdots$, where δT, $\delta^2 T$, ..., are the first variation, second variation, and so on, we obtain a power series in δV. The torus closure is completed when the fastest fragment meets the slowest one. These two particles are the extreme energy particles of the ensemble and have the following velocity increments: $\delta V_+ \overset{\text{def}}{=} \max\{\hat{V}\cdot\delta V\}$, $\delta V_- \overset{\text{def}}{=} \min\{\hat{V}\cdot V\}$ where $|\delta V_-| = |\delta V_+|$. The total difference in orbital period is $\Delta T \overset{\text{def}}{=} \Delta T(\delta V_+) - \Delta T(\delta V_-)$. This total difference is obtained by expanding the orbital difference in a Taylor series

$$\Delta T = \frac{\partial T}{\partial a}\frac{\partial a}{\partial V}\delta V + \frac{1}{2!}\left(\frac{\partial^2 T}{\partial a \partial V}\frac{\partial a}{\partial V} + \frac{\partial T}{\partial a}\frac{\partial^2 a}{\partial V^2}\right)\delta V^2 + \cdots \tag{5}$$

The partials are computed directly from the orbital period and the energy. The even variations of the total difference cancel out, and we end up with the approximation

$$\frac{\Delta T}{T} = 6\frac{a}{\mu}V\delta V_+ + \mathbb{O}\left(\frac{\delta V}{V}\right)^3 \tag{6}$$

Defining N_T as the number of revolutions for torus closure, and using the relation

$$\frac{\Delta T}{T}\cdot N_T = 1 \tag{7}$$

we obtain the following relation,

$$N_T = \frac{\mu}{6aV\delta V_+} + \mathbb{O}\left(\frac{\delta V}{V}\right) \tag{8}$$

which may be further simplified in the case of a small eccentricity

$$N_T \approx \frac{1}{6\delta V/V} + \mathbb{O}\left[e, \left(\frac{\delta V}{V}\right)\right] \tag{9}$$

Note that for a typical weak explosion[6] $\delta V/V = \mathbb{O}(10^{-2})$.

Figure 1 presents a map of the number of revolutions for torus closure as a function of the semimajor axis and the eccentricity. Two cases are considered: breakup at perigee and breakup at apogee. The corresponding number of revolutions are N_P and N_A, respectively. Increasing the semimajor axis results in fewer revolutions to complete the closure. Increasing the eccentricity reduces the number of revolutions for a perigee breakup but increases it for an apogee breakup, because N_T is inversely proportional to the orbital velocity at breakup.

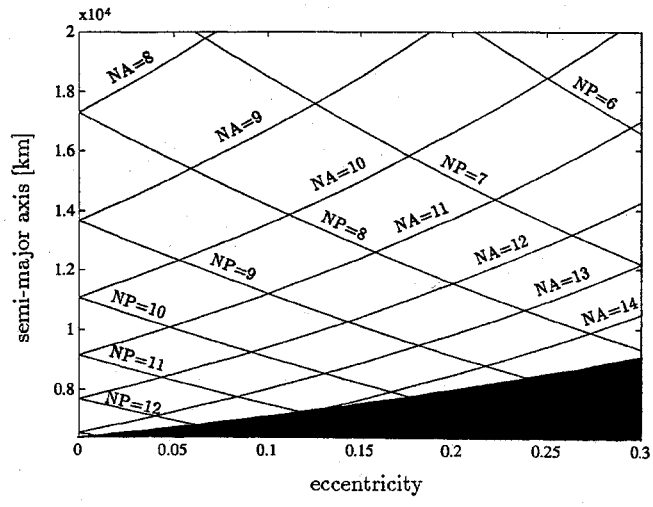

Fig. 1 Map for the torus closure.

To summarize this section, we have derived a simple formula for predicting the number of orbital revolutions from breakup to the torus closure. It is an approximate expression and is mostly accurate for a weak impulse.

III. Phase III: Apsidal and Nodal Closures

Consider the effects of the isotropic explosion on the propagation of the orbital elements under the influence of the Earth's oblateness. Since the relative impulse of breakup, $\delta V/V$, is much smaller than 1, we can expand the averaged orbital elements in $\delta V/V$. The first order of expansion consists of the following parts: the initial orbital elements, the small initial "jumps" due to the breakup impulse, the nominal secular precessing ellipse, and the variations in it due to the changes in *a, e,* and *i*. This model is represented by the following formulation,

$$\bar{\boldsymbol{a}}_j = \bar{\boldsymbol{a}}_0 + \dot{\bar{\boldsymbol{a}}}\,\Delta t + \delta\boldsymbol{a}_{0_j} + \delta\dot{\bar{\mathbf{a}}}_j\,\Delta t \tag{10}$$

where $\boldsymbol{a}$ denotes the vector of the orbital elements $\{a, e, i, M_0, \omega, \Omega\}$. Thanks to Poisson's formulation, the variations are a linear mapping of the impulse. Thus, the variations of the orbital elements of each particle j can be written as $\delta\boldsymbol{a}_j = \mathbf{S}\delta\boldsymbol{V}_j$. The 6×3, time-dependent matrix $\mathbf{S}$ will be named here as the sensitivity matrix and is given explicitly in the Appendix. The impulse is expressed in terms of the radial, transverse, and orthogonal components, $\delta\boldsymbol{V} = \{\delta V_r, \delta V_\theta, \delta V_w\}$. To summarize the model, the orbital elements of each particle are computed by applying the nominal secular precessing ellipse and the sensitivity matrix along the parent (nominal) orbit

$$\bar{\boldsymbol{a}}_j = \boldsymbol{a}_0 + \dot{\bar{\boldsymbol{a}}}\,\Delta t + \boldsymbol{S}\cdot\delta\boldsymbol{V}_j \tag{11}$$

Next, we wish to simplify this method to obtain tools for a fast prediction for the debris apsidal and nodal closures. The approach is to identify two couples of particles: the slowest and the fastest in terms of nodal and apsidal rates. Let us consider the relative apsidal and the relative nodal rates as a first-order approximation:

$$\delta\{\dot{\bar{\omega}}, \dot{\bar{\Omega}}\} = \frac{\partial\{\dot{\bar{\omega}}, \dot{\bar{\Omega}}\}}{\partial a}\delta a + \frac{\partial\{\dot{\bar{\omega}}, \dot{\bar{\Omega}}\}}{\partial e}\delta e + \frac{\partial\{\dot{\bar{\omega}}, \dot{\bar{\Omega}}\}}{\partial i}\delta i \tag{12}$$

Comparing the partials order of magnitude (Appendix) indicates that the order of $\partial\{\dot{\bar{\omega}}, \dot{\bar{\Omega}}\}/\partial e$ is $\mathbb{O}(e)$ relative to the order of the other partials. Therefore, the first-order approximation for a small eccentric orbit is

$$\delta\{\dot{\bar{\omega}}, \dot{\bar{\Omega}}\} \approx \frac{\partial\{\dot{\bar{\omega}}, \dot{\bar{\Omega}}\}}{\partial a}\delta a + \frac{\partial\{\dot{\bar{\omega}}, \dot{\bar{\Omega}}\}}{\partial i}\delta i \tag{13}$$

Now the changes of the semimajor axis and the eccentricity in Poisson's formulation can be approximated as $\delta a \approx (2/n)\,\delta V_\theta$ and $\delta i \approx (\cos u/na)\,\delta V_w$. It should be noted at this point that the couple of particles are probably ejected out of the orbital plane. The reason is the inclination in the oblateness disturbing function. For the purpose of identifying these particles, we express the impulse as $\delta V = \delta V \cos\beta\hat{e}_\theta + \delta V \sin\beta\hat{e}_w$, where $\hat{e}_\theta$ and $\hat{e}_w$ represent the transverse and the orthogonal direction and β measures the out-of-plane angle of the projected particles. Note that the radial component was omitted because we have assumed a small eccentricity. It can be neglected as well in eccentric orbits if the breakup occurs near the perigee or the apogee, as easily seen from Poisson's formulation. The final expression for the relative apsidal rate for a particle ejected with the impulse $\{\delta V, \beta\}$ is

$$\delta\dot{\bar{\omega}} \approx -\frac{3}{2}J_2\frac{R_\otimes^2}{a^3} \times\left[7\left(2-\frac{5}{2}\sin^2 i\right)\cos\beta + \frac{5}{2}\sin 2i\cos\mu\sin\beta\right]\delta V \tag{14}$$

Evaluating the extremum of $\delta\dot{\bar{\omega}}$ with respect to β gives the direction corresponding to the fastest relative apsidal rate

$$\tan\beta = \frac{5\sin 2i\cos u}{14\,(2-\frac{5}{2}\sin^2 i)} \tag{15}$$

A similar procedure leads to the relative nodal closure

$$\delta\dot{\bar{\Omega}} \approx \frac{3}{2}J_2\frac{R_\otimes^2}{a^3}\left(7\cos i\cos\beta + \sin i\cos u\sin\beta\right)\delta V \tag{16}$$

which is maximal at

$$\tan\beta = 1/7\tan i\cos u \tag{17}$$

The two couples (apsidal and nodal) are in a phase of 180 deg. Thus, the differences between the fastest and the slowest drifts are $\Delta\{\dot{\bar{\omega}}, \dot{\bar{\Omega}}\} = 2\{|\delta\dot{\bar{\omega}}|, |\delta\dot{\bar{\Omega}}|\}$, and the times for apsidal and nodal closures are

$$\{T_\omega, T_\Omega\} = \frac{\pi}{\Delta\{\dot{\bar{\omega}}, \dot{\bar{\Omega}}\}} \tag{18}$$

Figure 2 describes the relative nodal rate as a function of the ejection angle for various inclinations and for $u = 0$ deg. The dotted line indicates the maximal relative nodal rate. It shows the deviation of the ejection angle for $\delta\dot{\bar{\Omega}}_{max}$ from the orbital plane. The maximal energy solution (the vertical axis) matches only the single case of an equatorial orbit. Note that the current figure corresponds to an explosion at the ascending node.

Figure 3 shows the influence of the breakup location (ascending node, pole, and descending node). The solutions for the maximal relative nodal rates are symmetrical with respect to $u=0$, in which the solution is identical with the maximal energy solution. The nodal closure is mainly affected by the inclination. The time for nodal closure in equatorial orbits is at least one order of magnitude faster than the closure time in polar orbits.

In summary of this section, two couples of particles that define the apsidal and the nodal closures, have been identified. A closed-form expression for the typical times of phase III are straightforward byproducts.

IV. Conditions for Phase IV

An idealistic approach for dealing with the current phase is to separate it from the previous phase. This means that the fourth phase starts after a complete nodal and apsidal dispersion. In other words, the oblateness and the atmospheric perturbations are never acting together. However, in certain cases both perturbations are in the same order of magnitude. Then the approach of separation fails, and we must deal with the rather complicated transition process.

In this section, we wish to find a simple criterion for the set of parameters that allows (approximately) the separation between phases III and IV. We start with phase IV and assume that phase III has been completed. An additional assumption of small eccentricity leads to the following solvable equation for the orbital decay:

$$\frac{da}{dt} = -\frac{A}{m}C_D\rho\sqrt{\mu a} \tag{19}$$

Since the semimajor axis is a slow variable, the orbital decay Δa can be restricted such that $\Delta a/a \ll 1$. The first-order approximate solution is

$$\Delta a \simeq -\frac{A}{m}C_D\rho\sqrt{\mu a}(t-t_0) \tag{20}$$

The decay time order is a matter of definition and should be determined according to the user criterion for the maximal orbital decay. Let Δa_{max} be such a decay; then the corresponding time order for phase IV is

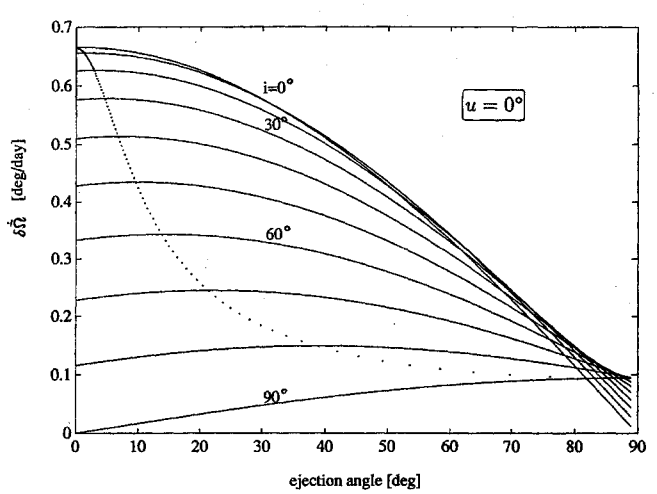

Fig. 2 Maximal relative nodal rates.

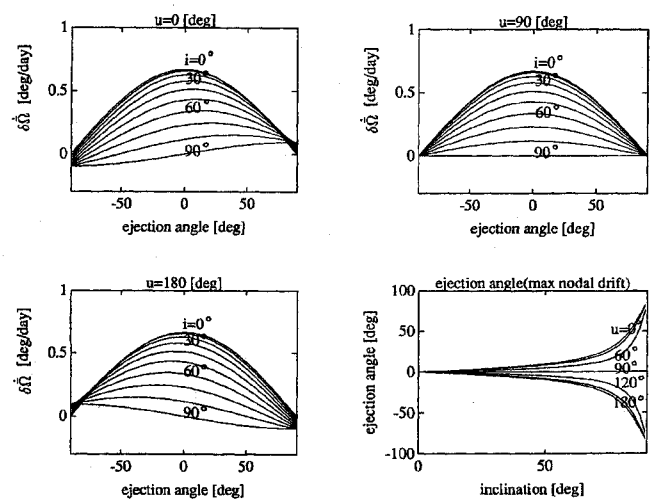

Fig. 3 Maps for the relative nodal rate.

$$\delta\{\dot{\bar{\omega}}, \dot{\bar{\Omega}}\} \approx \frac{\partial\{\dot{\bar{\omega}}, \dot{\bar{\Omega}}\}}{\partial a}\delta a + \frac{\partial\{\dot{\bar{\omega}}, \dot{\bar{\Omega}}\}}{\partial i}\delta i \tag{13}$$

Now the changes of the semimajor axis and the eccentricity in Poisson's formulation can be approximated as $\delta a \approx (2/n)\,\delta V_\theta$ and $\delta i \approx (\cos u/na)\,\delta V_w$. It should be noted at this point that the couple of particles are probably ejected out of the orbital plane. The reason is the inclination in the oblateness disturbing function. For the purpose of identifying these particles, we express the impulse as $\delta V = \delta V \cos\beta\hat{e}_\theta + \delta V \sin\beta\hat{e}_w$, where $\hat{e}_\theta$ and $\hat{e}_w$ represent the transverse and the orthogonal direction and β measures the out-of-plane angle of the projected particles. Note that the radial component was omitted because we have assumed a small eccentricity. It can be neglected as well in eccentric orbits if the breakup occurs near the perigee or the apogee, as easily seen from Poisson's formulation. The final expression for the relative apsidal rate for a particle ejected with the impulse $\{\delta V, \beta\}$ is

$$\delta\dot{\bar{\omega}} \approx -\frac{3}{2}J_2\frac{R_\otimes^2}{a^3} \times \left[7\left(2 - \frac{5}{2}\sin^2 i\right)\cos\beta + \frac{5}{2}\sin 2i\cos\mu\sin\beta\right]\delta V \tag{14}$$

Evaluating the extremum of $\delta\dot{\bar{\omega}}$ with respect to β gives the direction corresponding to the fastest relative apsidal rate

$$\tan\beta = \frac{5\sin 2i\cos u}{14\,(2 - 5/2\sin^2 i)} \tag{15}$$

A similar procedure leads to the relative nodal closure

$$\delta\dot{\bar{\Omega}} \approx \frac{3}{2}J_2\frac{R_\otimes^2}{a^3}\left(7\cos i\cos\beta + \sin i\cos u\sin\beta\right)\delta V \tag{16}$$

which is maximal at

$$\tan\beta = 1/7\tan i\cos u \tag{17}$$

The two couples (apsidal and nodal) are in a phase of 180 deg. Thus, the differences between the fastest and the slowest drifts are $\Delta\{\dot{\bar{\omega}}, \dot{\bar{\Omega}}\} = 2\{|\delta\dot{\bar{\omega}}|, |\delta\dot{\bar{\Omega}}|\}$, and the times for apsidal and nodal closures are

$$\{T_\omega, T_\Omega\} = \frac{\pi}{\Delta\{\dot{\bar{\omega}}, \dot{\bar{\Omega}}\}} \tag{18}$$

Figure 2 describes the relative nodal rate as a function of the ejection angle for various inclinations and for $u = 0$ deg. The dotted line indicates the maximal relative nodal rate. It shows the deviation of the ejection angle for $\delta\dot{\bar{\Omega}}_{max}$ from the orbital plane. The maximal energy solution (the vertical axis) matches only the single case of an equatorial orbit. Note that the current figure corresponds to an explosion at the ascending node.

Figure 3 shows the influence of the breakup location (ascending node, pole, and descending node). The solutions for the maximal relative nodal rates are symmetrical with respect to u=0, in which the solution is identical with the maximal energy solution. The nodal closure is mainly affected by the inclination. The time for nodal closure in equatorial orbits is at least one order of magnitude faster than the closure time in polar orbits.

In summary of this section, two couples of particles that define the apsidal and the nodal closures, have been identified. A closed-form expression for the typical times of phase III are straightforward byproducts.

IV. Conditions for Phase IV

An idealistic approach for dealing with the current phase is to separate it from the previous phase. This means that the fourth phase starts after a complete nodal and apsidal dispersion. In other words, the oblateness and the atmospheric perturbations are never acting together. However, in certain cases both perturbations are in the same order of magnitude. Then the approach of separation fails, and we must deal with the rather complicated transition process.

In this section, we wish to find a simple criterion for the set of parameters that allows (approximately) the separation between phases III and IV. We start with phase IV and assume that phase III has been completed. An additional assumption of small eccentricity leads to the following solvable equation for the orbital decay:

$$\frac{da}{dt} = -\frac{A}{m}C_D\rho\sqrt{\mu a} \tag{19}$$

Since the semimajor axis is a slow variable, the orbital decay Δa can be restricted such that $\Delta a/a \ll 1$. The first-order approximate solution is

$$\Delta a \approx -\frac{A}{m}C_D\rho\sqrt{\mu a}(t - t_0) \tag{20}$$

The decay time order is a matter of definition and should be determined according to the user criterion for the maximal orbital decay. Let Δa_{max} be such a decay; then the corresponding time order for phase IV is

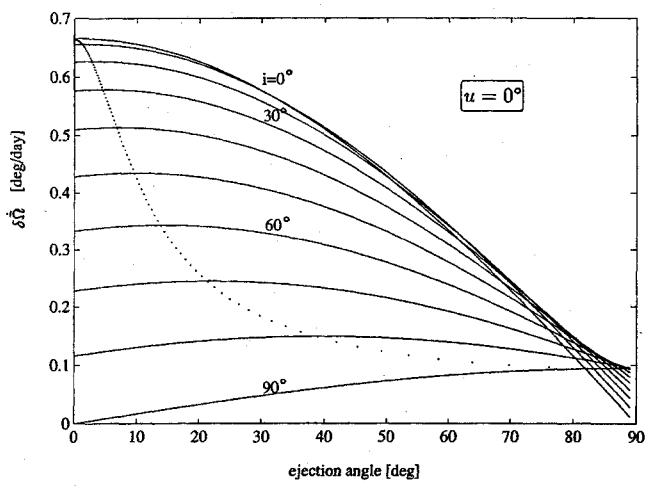

Fig. 2 Maximal relative nodal rates.

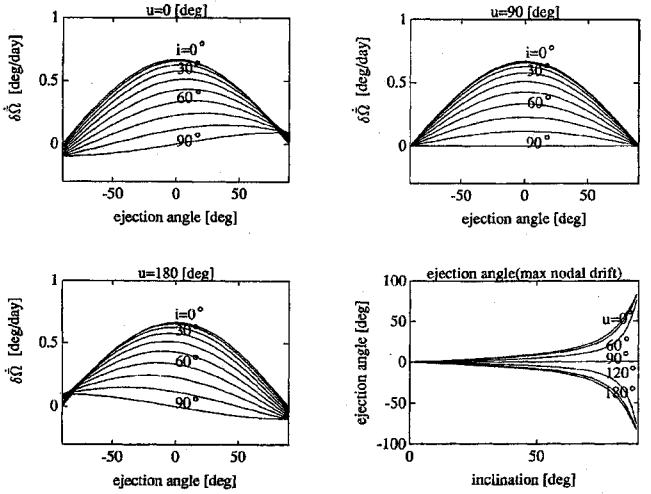

Fig. 3 Maps for the relative nodal rate.

$$\tau_D = \frac{\Delta a_{max}/a}{A/mC_D\rho V} \tag{21}$$

On the other hand, we regard the time for the different drift rates to complete a nodal closure as the time order of phase III

$$\tau_\Omega \equiv T_\Omega = \frac{2\pi}{3J_2 n(R_\otimes/a)^2\,|f(i,u)|\,(\delta V/V)} \tag{22}$$

where

$$f = (7\cos i\cos\beta + \sin i\cos u\sin\beta)\,|_{\max\{\beta\}} \tag{23}$$
$$= 7\cos i\sqrt{1 + 1/49\tan^2 i\cos^2 u}$$

Comparing both time orders, it is useful to define the following nondimensional number S, named the band number:

$$S \overset{\text{def}}{=} \frac{2\pi(A/m)C_D\rho V}{21J_2 n(R_\otimes/a)^2\cos i\sqrt{1 + (1/49)\tan^2 i\cos^2 u}(\delta a_{max}/a)}$$
$$\equiv \frac{\tau_\Omega}{\tau_D}\cdot\frac{\delta V}{V} \tag{24}$$

The completeness of the band closure is guaranteed if

$$S \ll \frac{\delta V}{V} \tag{25}$$

which is equivalent to $\tau_D \gg \tau_\Omega$.

Figure 4 describes the band number as a function of the altitude H and the ballistic ratio A/m. The criterion for the decay time order was chosen such that $\Delta a_{max}/a = 0.1$. The band number is compared with several impulses for indicating the sets of parameters that give rise to a band closure.

In summarizing this section, we have defined the band number, which helps us set the limits between phases III and IV. The two phases can be dealt with separately if the breakup impulse is much greater than the band number, only after a few hundred days (the time order of the band closure) that the dissipation has to be considered.

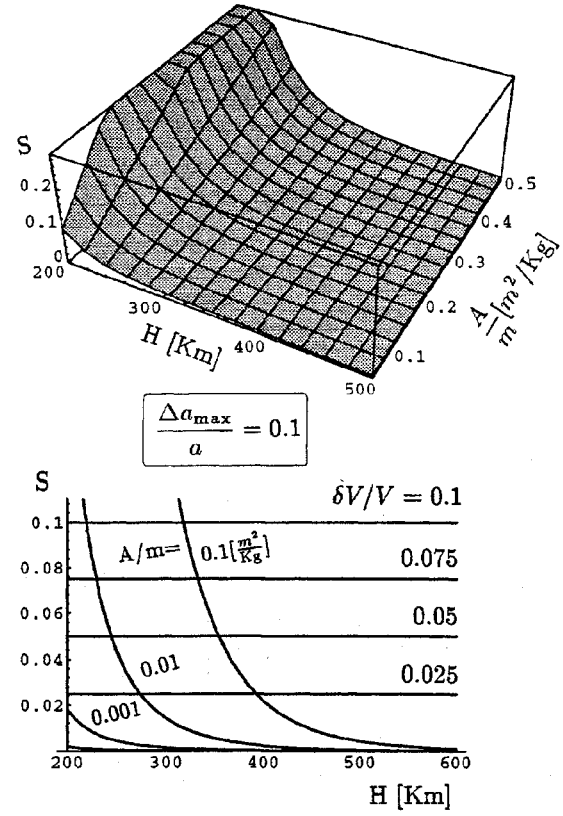

Fig. 4 Band number.

V. Concluding Remarks

Simple procedures to estimate the debris orbital, apsidal, and nodal closures have been developed. These handy formulas save the need for a heavy numerical integration for each particle and enable the user to obtain a quick prediction of the time order for each phase. An explosion at perigee gives rise to a faster torus closure than an apogee explosion. It was found that the fastest and slowest relative apsidal and nodal rates are not dominated by the extreme energy particles. The orientation of these particles is mostly a function of the orbital inclination. To eliminate the mixing between phases III and IV, the band number is defined. It decreases with the altitude and increases with the ballistic ratio. Small values of this number, compared with the impulse strength, guarantee the completeness of the nodal dispersion.

It is essential to notice that the mechanism of the breakup is unpredictable; therefore the impulse strength is a random input that needs to be estimated before applying it to the current model. It is also important to mention that this paper was not intended to present a comprehensive solution to all aspects of the propagation phases. The goal of this research was the development of tools for a preliminary prediction, in other words, a "first shoot." The next step is the more exact computation of the ensemble density propagation in phases II, III, and IV. This remains an unsolved problem and a challenging subject for future research.

Appendix

The complete expression for the sensitivity matrix is given by the following time-dependent matrix. The partials are presented in Table A1 and are separated into two groups: those related to the breakup (impulse) and those related to the secular precessing ellipse.

$$\mathbf{S} = \begin{matrix} \frac{\partial a_0}{\partial V_r} & \frac{\partial a_0}{\partial V_\theta} & 0 \\ \frac{\partial e_0}{\partial V_r} & \frac{\partial e_0}{\partial V_\theta} & 0 \\ 0 & 0 & \frac{\partial i_0}{\partial V_w} \end{matrix}$$

$$\begin{matrix} \frac{\partial M_0}{\partial V_r} + \left(\frac{\partial \bar{n}}{\partial a}\frac{\partial a_0}{\partial V_r} + \frac{\partial \bar{n}}{\partial e}\frac{\partial e_0}{\partial V_r}\right)\Delta t & \frac{\partial M_0}{\partial V_\theta} + \left(\frac{\partial \bar{n}}{\partial a}\frac{\partial a_0}{\partial V_\theta} + \frac{\partial \bar{n}}{\partial e}\frac{\partial e_0}{\partial V_\theta}\right)\Delta t & \frac{\partial \bar{n}}{\partial i}\frac{\delta i_0}{\partial V_w}\Delta t \\ \frac{\partial \omega_0}{\partial V_r} + \left(\frac{\partial \dot{\bar{\omega}}}{\partial a}\frac{\partial a_0}{\partial V_r} + \frac{\partial \dot{\bar{\omega}}}{\partial e}\frac{\partial e_0}{\partial V_r}\right)\Delta t & \frac{\partial \omega_0}{\partial V_\theta} + \left(\frac{\partial \dot{\bar{\omega}}}{\partial a}\frac{\partial a_0}{\partial V_\theta} + \frac{\partial \dot{\bar{\omega}}}{\partial e}\frac{\partial e_0}{\partial V_\theta}\right)\Delta t & \frac{\partial \omega_0}{\partial V_w} + \frac{\partial \dot{\bar{\omega}}}{\partial i}\frac{\partial i_0}{\partial V_w}\Delta t \\ \left(\frac{\partial \dot{\bar{\Omega}}}{\partial a}\frac{\partial a_0}{\partial V_r} + \frac{\partial \dot{\bar{\Omega}}}{\partial e}\frac{\partial e_0}{\partial V_r}\right)\Delta t & \left(\frac{\partial \dot{\bar{\Omega}}}{\partial a}\frac{\partial a_0}{\partial V_\theta} + \frac{\partial \dot{\bar{\Omega}}}{\partial e}\frac{\partial e_0}{\partial V_\theta}\right)\Delta t & \frac{\partial \Omega_0}{\partial V_w} + \frac{\partial \dot{\bar{\Omega}}}{\partial i}\frac{\partial i_0}{\partial V_w}\Delta t \end{matrix}$$

Table A1 The partials for the sensitivity matrix

Impulse	Secular precessing ellipse
$\frac{\partial a}{\partial V_r} = \frac{2e \sin \vartheta}{n\tilde{b}^{1/2}}$	$\frac{\partial \bar{n}}{\partial a} = -\frac{3n_0}{2a}\left[1 + \frac{7}{2}J_2\left(\frac{R_\oplus}{a}\right)^2 \tilde{b}^{-3/2}\left(1 - \frac{3}{2}\sin^2 i\right)\right]$
$\frac{\partial a}{\partial V_\theta} = \frac{2(1 + e\cos \vartheta)}{n\tilde{b}^{1/2}}$	$\frac{\partial \bar{n}}{\partial e} = \frac{9}{2} n_0 J_2\left(\frac{R_\oplus}{a}\right)^2 e\tilde{b}^{-5/2}\left(1 - \frac{3}{2}\sin^2 i\right)$
$\frac{\partial e}{\partial V_r} = \frac{\tilde{b}^{1/2}\sin \vartheta}{na}$	$\frac{\partial \bar{n}}{\partial i} = -\frac{9}{4} n_0 J_2\left(\frac{R_\oplus}{a}\right)^2 \tilde{b}^{-3/2}\sin 2i$
$\frac{\partial e}{\partial V_\theta} = \frac{\tilde{b}^{1/2}[2\cos \vartheta + (1 + \cos^2 \vartheta)e]}{na(1 + e\cos \vartheta)}$	$\frac{\partial \dot{\bar{\omega}}}{\partial a} = \frac{3}{2} J_2 \frac{R_\oplus^2}{a^3}\tilde{b}^{-2}\left(2 - \frac{5}{2}\sin^2 i\right)\left(-2\bar{n} + a\frac{\partial \bar{n}}{\partial a}\right)$
$\frac{\partial i}{\partial V_w} = \frac{\tilde{b}^{1/2}\cos(\omega + \vartheta)}{na(1 + e\cos \vartheta)}$	$\frac{\partial \dot{\bar{\omega}}}{\partial e} = \frac{3}{2} J_2\left(\frac{R_\oplus}{a}\right)^2 \tilde{b}^{-3}\left(2 - \frac{5}{2}\sin^2 i\right)\left[4e\bar{n} + \tilde{b}\frac{\partial \bar{n}}{\partial e}\right]$
$\frac{\partial M_0}{\partial V_r} = \frac{\tilde{b}}{nae}\left(\cos \vartheta - \frac{2e}{1 + e\cos \vartheta}\right)$	$\frac{\partial \dot{\bar{\omega}}}{\partial i} = \frac{3}{2} J_2\left(\frac{R_\oplus}{a}\right)^2 \tilde{b}^{-2}\left[-\frac{5}{2}\bar{n}\sin 2i + \left(2 - \frac{5}{2}\sin^2 i\right)\frac{\partial \bar{n}}{\partial i}\right]$
$\frac{\partial M_0}{\partial V_\theta} = -\frac{\tilde{b}(2 + e\cos \vartheta)\sin \vartheta}{nae(1 + e\cos \vartheta)}$	$\frac{\partial \dot{\bar{\Omega}}}{\partial a} = \frac{3}{2} J_2 \frac{R_\oplus^2}{a^3}\tilde{b}^{-2}\cos i\left(2\bar{n} - a\frac{\partial \bar{n}}{\partial a}\right)$
$\frac{\partial \omega}{\partial V_r} = -\frac{\tilde{b}^{1/2}\cos \vartheta}{nae}$	$\frac{\partial \dot{\bar{\Omega}}}{\partial e} = -\frac{3}{2} J_2\left(\frac{R_\oplus}{a}\right)^2 \tilde{b}^{-3}\cos i\left[4e\bar{n} + \tilde{b}\frac{\partial \bar{n}}{\partial e}\right]$
$\frac{\partial \omega}{\partial V_\theta} = \frac{\tilde{b}^{1/2}(2 + e\cos \vartheta)\sin \vartheta}{nae(1 + e\cos \vartheta)}$	$\frac{\partial \dot{\bar{\Omega}}}{\partial i} = \frac{3}{2} J_2\left(\frac{R_\oplus}{a}\right)^2 \tilde{b}^{-2}\left(\bar{n}\sin i - \cos i\frac{\partial \bar{n}}{\partial i}\right)$
$\frac{\partial \omega}{\partial V_w} = -\frac{\tilde{b}^{1/2}\sin(\omega + \vartheta)\cot i}{na(1 + e\cos \vartheta)}$	
$\frac{\partial \Omega}{\partial V_w} = \frac{\tilde{b}^{1/2}\sin(\omega + \vartheta)}{na(1 + e\cos \vartheta)\sin i}$	where $\tilde{b} \stackrel{\text{def}}{=} 1 - e^2$

References

[1] Jehn, R., "Dispersion of Debris Cloud from In-Orbit Fragmentation Events," *ESA Journal,* Vol. 15, No. 1, 1991, pp. 63–77.

[2] Ashenberg, J., "On the Short-Term Spread of Space Debris," AIAA Paper 92-4441, Aug. 1992.

[3] Battin, R. H., *An Introduction to the Mathematics and Methods of Astrodynamics,* AIAA Educational Series, New York, 1987, pp. 496, 497.

[4] Meirovitch, L., *Methods of Analytical Dynamics,* MaGraw-Hill, New York, 1970, p. 456.

[5] Escobal, P. R. E., *Methods of Orbit Determination,* Krieger Publishing, Malabar, FL, 1965, pp. 384, 385.

[6] Chobotov, V. A., "Dynamics of Orbital Debris Clouds and the Resulting Collision Hazard to Spacecraft," *Journal of the British Interplanetary Society,* Vol. 43, May 1990, pp. 187–195.

[7] Chobotov, V. A., Spencer, D. B., Schmitt, D. L., Gupta, R. P., Hopkins, R. G., and Knapp, D. T., "Dynamics of Debris Motion and the Collision Hazard to Spacecraft Resulting from an Orbital Breakup," The Aerospace Corporation, SD-TR-88-96, El Segundo, CA, Jan. 1988.

[8] Ashenberg, J., and Broucke, R. A., "The Effect of the Earth's Oblateness on the Long-Term Dispersion of Debris," *Advanced Space Research* (to be published).

[9] Ross, S., "The Orbital Motion of Pellet Clouds," *The Journal of the Astronautical Sciences,* Vol. 8, No. 3, 1961, pp. 79–82.